

# Néel temperature dependence of Cr + 1 at.% Al thin films on MgO(110), MgO(100) and fused silica

ZP Mudau<sup>1</sup>, ARE Prinsloo<sup>1</sup>, CJ Sheppard<sup>1</sup>, AM Venter<sup>2</sup> and EE Fullerton<sup>3</sup>

<sup>1</sup>Department of Physics, University of Johannesburg, PO Box 524, Auckland Park, 2006, South Africa

<sup>2</sup>Research and Development Division, Necsa Limited SOC, P.O. Box 582, Pretoria 0001, South Africa

<sup>3</sup>Center for Magnetic Recording Research, University of California, San Diego, 9500 Gilman Dr., La Jolla, CA 92093-0401, USA

Author e-mail address: cjsheppard@uj.ac.za

**Abstract.** We have investigated the magnetic and transport properties Cr<sub>99</sub>Al<sub>1</sub> films of thickness ( $t$ ) from 28 to 450 nm deposited on fused silica, MgO(100) and MgO(110) by DC magnetron sputtering. The x-ray diffraction results were used to determine the crystallographic orientation of the thin films and the Néel transition temperature,  $T_N$ , was obtained using standard four-point probe resistance ( $R$ ) measurements as function of temperature ( $T$ ). Results show polycrystalline structure for sample prepared on fused silica while those on MgO(100) and MgO(110) shows good epitaxial growth. For samples deposited on fused silica no anomalies associated with the  $T_N$  were observed in  $R(T)$ . The  $R(T)$  curves for films deposited on MgO substrates showed anomalies associated with  $T_N$  shaped as weak domes. The  $T_N$  values decreased with increase in  $t$ , levelling off at approximately 260 K for the 452 nm sample. This correlates with the  $T_N$  value expected from the magnetic phase diagram of bulk Cr-Al for this concentration.

## 1. Introduction

Chromium is an itinerant-electron antiferromagnetic (AFM) element which has an incommensurate spin density wave (ISDW) below the Néel transition temperature ( $T_N$ ) of 311 K [1]. The unique characteristic of the spin density wave (SDW) is a result of the nesting between the electron and hole Fermi surfaces [1]. Cr alloys weakly diluted with metals retain their antiferromagnetism, but can have magnetic properties different to that of pure Cr. This is strongly dependant on the nature and concentration of the dilute [1]. Cr has an electron-to-atom ( $e/a$ ) ratio of six. Alloying Cr with metals with different  $e/a$  values, affects the relative sizes of the electron and hole Fermi surfaces which in turn influences their nesting in the AFM phase. As the AFM nature of the Cr alloys are directly linked to the nesting of the Fermi surfaces, the effects are clearly seen in a variety of physical properties [1]. Alloying Cr with elements with an  $e/a$  less than six, such as V (with an  $e/a = 5$ ), normally results in a decrease in  $T_N$  with the increase in diluent concentration, while alloying Cr with elements with  $e/a$  larger than six such as Mn

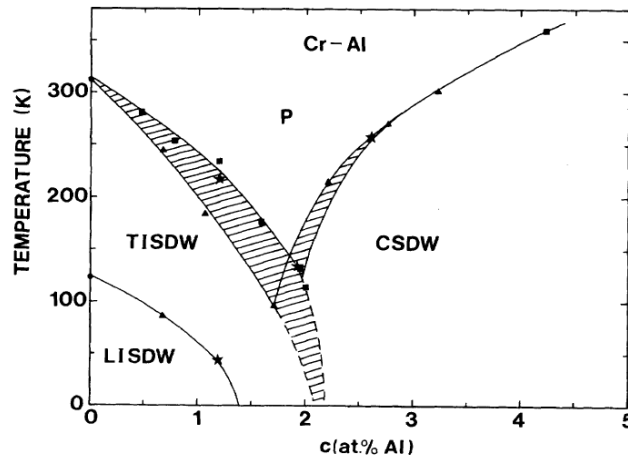


**Figure 1:** Concentration-Temperature ( $c$ - $T$ ) magnetic phase diagram of bulk Cr-Al alloy system that summarises the existence of three different spin density wave phases at a triple point around 2 at. % Al and 130 K, where the incommensurate spin density wave (ISDW), commensurate spin density wave (CSDW) and paramagnetic (P) phases coexist [3]. TISDW indicates the existence of a transverse polarised ISDW phase and LISDW a longitudinal polarised ISDW phase.

(with an  $e/a = 7$ ) normally results in an increased  $T_N$  with increase in diluent concentration [1]. Cr-Al is an exception to this general rule. Aluminium (with  $e/a = 3$ ) does not give a continuous decrease of  $T_N$  with increase in dilute concentration as expected, but instead the magnetic phase diagram shows a deep minimum around 2 at.% Al after which  $T_N$  increases sharply with further increase in concentration, as indicated in Figure 1. The origin of this unique behaviour in Cr-Al has been the subject of many studies [1, 2], but no conclusion has been reached in this regard.

At present there is no quantitative agreement in the literature concerning the position and the depth of the minimum [2, 3]. The  $c$ - $T$  magnetic phase diagram also reveals the existence of three spin density wave phases converging to a triple point around 2 at.% Al and 130 K where all three phases coexist [2, 3]. The phase diagram shows the presence of an ISDW structure at 1 at.% Al, with a transition from longitudinal to transverse ISDW at a temperature of approximately 60 K [3]. In addition a recent study suggests that the triple point occurs at 2.2 at.% Al and 0 K; and most interestingly implies that this triple point may also be a quantum critical point [5].

Thin films of Cr alloys have shown unique properties not observed in bulk material [4]. Their magnetic properties are strongly influenced by the film thickness, surface and proximity magnetic effects. This study now extends such investigations to include  $\text{Cr}_{99}\text{Al}_1$  thin films of different thicknesses deposited on different substrates.

## 2. Experimental

The Cr-Al thin films were prepared using DC magnetron sputtering at a substrate temperature of 973 K and argon pressure 3 mTorr, from elemental sources onto single-crystal MgO(110) and MgO(100), as well as fused silica substrates. The sample was prepared at a fixed concentration of Cr + 1 at.% Al with thicknesses from 28 to 452 nm. The film thickness was controlled through varying deposition rates and times and confirmed using x-ray diffraction (XRD) techniques. In order to investigate the growth orientation of the thin films symmetrical  $\theta$ - $2\theta$  XRD was done using the Bragg-Brentano configuration set-up on Phillips X'Pert Pro Diffractometer. Electrical resistance measurements from 77 to 400 K using the standard DC four-probe method were employed to determine the Néel transition temperatures of these samples.

### 3. Results

Figures 2(a) to (c) summarise the representative XRD results for the  $\text{Cr}_{99}\text{Al}_1$  thin films deposited on single crystalline  $\text{MgO}(110)$  with  $t = 452$  nm,  $\text{MgO}(100)$  with  $t = 226$  nm and polycrystalline fused silica with  $t = 226$  nm, respectively. The XRD results indicate that all the samples prepared on  $\text{MgO}(100)$  and  $\text{MgO}(110)$  are epitaxial and exhibit a single crystallographic orientation, with the  $\text{Cr}_{99}\text{Al}_1$  layers showing preferred growth direction of (100) and (211). Thin films prepared on fused silica substrates have a polycrystalline structure with no preferred orientation. The Néel temperature ( $T_N$ ) of the films were determined from anomalies observed in the electrical resistance ( $R$ ) measurements as a function of temperature ( $T$ ). Representative  $R$ - $T$  curves are shown in Figure 3 for samples deposited on (a)  $\text{MgO}(110)$  with  $t = 226$  nm, (b)  $\text{MgO}(100)$  with  $t = 226$  nm and (c) fused silica with  $t = 226$  nm.

Resistivity results of thin films prepared on  $\text{MgO}(100)$  and  $\text{MgO}(110)$  substrates show anomalies in the shape of weak domes that are ascribed to the formation of the ISDW on cooling down from the paramagnetic phase.  $T_N$  is usually taken at the inflection point of  $R - T$  curves, but since the anomaly is relatively weak in the  $\text{Cr}_{99}\text{Al}_1$  thin films, this point is determined from the  $dR/dT$  versus  $T$  curve which is calculated from the  $R - T$  data. An example of such a curve is shown in Figure 3 (d) and  $T_N$  is taken at the temperature associated with the minimum. This is the standard method used to determine the  $T_N$  of Cr thin films [8]. However, it should be mentioned that the  $T_N$  values obtained maybe biased to some extent due to the extrinsic morphology contribution that dramatically changes the resistance [8]. No evidence is seen of the TISDW to LISDW phase transition in the  $R$ - $T$  curves at low temperatures [1, 2], as was observed in bulk Cr-Al single crystals and reflected in Figure 1.

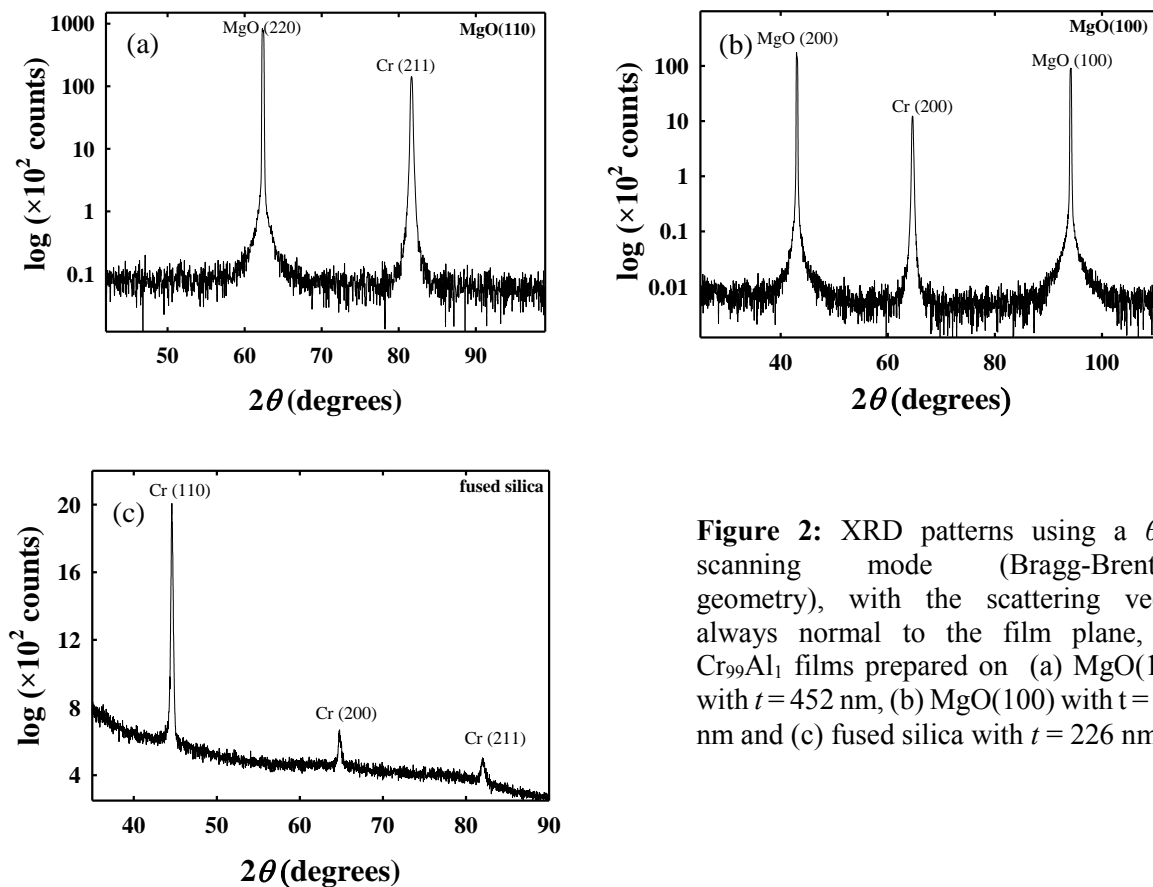


**Figure 2:** XRD patterns using a  $\theta$ - $2\theta$  scanning mode (Bragg-Brentano geometry), with the scattering vector always normal to the film plane, for  $\text{Cr}_{99}\text{Al}_1$  films prepared on (a)  $\text{MgO}(110)$  with  $t = 452$  nm, (b)  $\text{MgO}(100)$  with  $t = 226$  nm and (c) fused silica with  $t = 226$  nm.

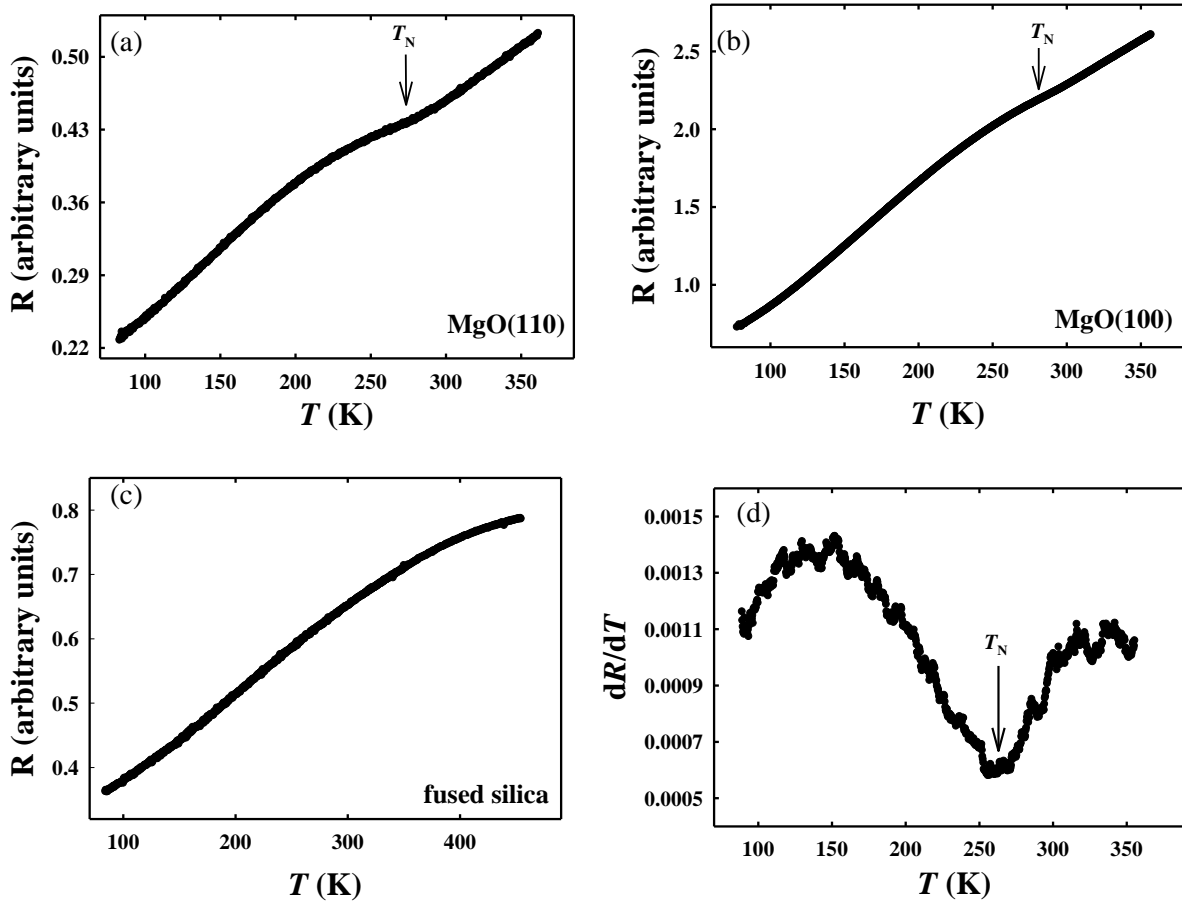


**Figure 3:** Resistance ( $R$ ) versus temperature ( $T$ ) graphs for  $\text{Cr}_{99}\text{Al}_1$  thin films prepared on (a)  $\text{MgO}(110)$  with  $t = 226$  nm, (b)  $\text{MgO}(100)$  with  $t = 46.5$  nm, (c) fused silica with  $t = 226$  nm and (d) show  $dR/dT$  versus  $T$  for the  $\text{MgO}(110)$  with  $t = 226$  nm sample. The temperature associated with the minimum in the  $dR/dT$  versus  $T$  curves was taken as the  $T_N$ .

For  $\text{Cr}_{99}\text{Al}_1$  thin films deposited on fused silica no anomalies were observed in the temperature range of 77 to 400 K. The  $T_N$  seemed to be higher than 400 K, from Figure 3 (c) it is clear there is a sudden increase of  $R$ , but the inflection point where it started to increase it is not observed in the measured temperature range. Measurements at higher temperatures were not considered as the experimental presently available in the laboratories did not allow for measurements under high vacuum and this can result in a permanent physical damage of the thin films – in the form of sample peeling and oxidation.

Figure 4 shows the variation of  $T_N$  as a function of thickness ( $t$ ) for the samples prepared on  $\text{MgO}(110)$  and  $\text{MgO}(100)$  substrates. For epitaxial thin films prepared on  $\text{MgO}(110)$ , there is a slight increase in  $T_N$  with the increase in thickness, reaching a maximum around 280 K, followed by a decrease and then levelling off at approximately 260 K as shown in Figure 4 (a). For the  $\text{Cr}_{99}\text{Al}_1$  epitaxial thin films prepared on  $\text{MgO}(100)$ , the  $T_N$  is decreases with increase in  $t$  from around 290 K, giving rise to a minimum at  $t = 80$  nm with the lowest  $T_N$  value of 245 K, finally levelling off at approximately 260 K for the thickest samples. The  $T_N$  values obtained for the  $\text{Cr}_{99}\text{Al}_1$  thin films with  $t > 200$  nm on  $\text{MgO}(110)$  and  $\text{MgO}(100)$  substrates is in agreement with what is expected from the  $c$ - $T$  magnetic phase diagram

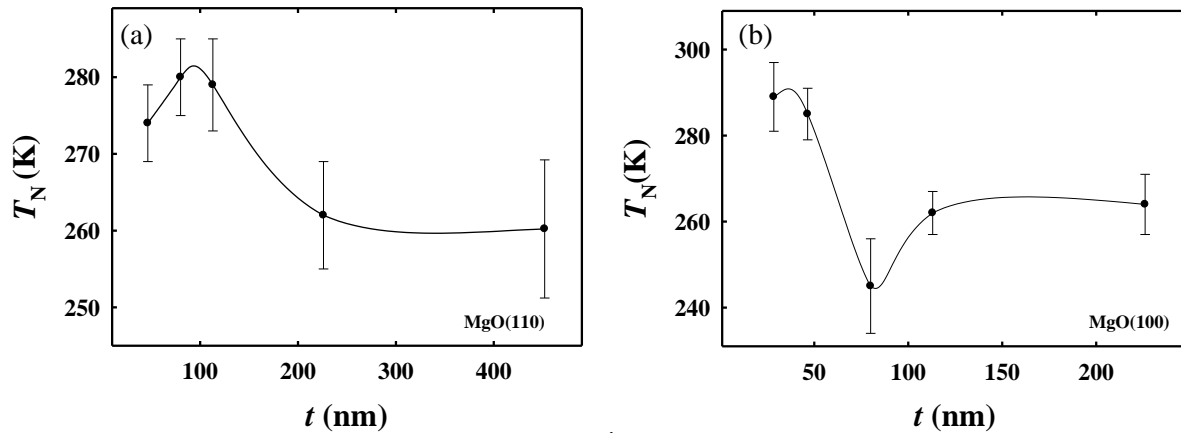


**Figure 4:**  $T_N$  versus  $\text{Cr}_{99}\text{Al}_1$  layer thickness ( $t$ ) as prepared on the substrates (a)  $\text{MgO}(110)$  and (b)  $\text{MgO}(100)$ .

of bulk Cr-Al. The  $c$ - $T$  magnetic phase diagram shows  $T_N$  to be around 240 to 260 K for bulk Cr + 1 at.% Al.

It is noted that the behaviour of  $T_N - t$  for the  $\text{Cr}_{99}\text{Al}_1$  sample series prepared on  $\text{MgO}(110)$  and  $\text{MgO}(100)$  differs slightly as the  $T_N$  values levels off at  $t > 200$  nm for the  $\text{MgO}(110)$  series, but this levelling off already happens at  $t > 100$  nm for the  $\text{MgO}(100)$  series. This might be attributed to the different crystallographic orientations obtained for the  $\text{Cr}_{99}\text{Al}_1$  thin films prepared on the various substrates [4]. Previous studies also linked growth morphology to the behaviour of  $T_N - t$  [6], this can be probed in further studies using AFM. Present results indicate that dimensionality strongly influence the  $T_N$  values in  $\text{Cr}_{99}\text{Al}_1$ . It is evident that the  $T_N$  values for samples prepared on  $\text{MgO}(110)$  is higher in the samples with  $t < 200$  nm than the values reflected in phase diagram shown in Figure 1 for bulk Cr-Al. This is also the case for the samples with  $t < 100$  nm prepared on  $\text{MgO}(100)$ . This can be attributed to higher stress and strain in the thinner films [7]. For the thicker films the values of  $T_N$  is in agreement with those reflected in Figure 1, obtained for bulk  $\text{Cr}_{99}\text{Al}_1$ , as expected [4].

The proposal that the  $T_N$  values for the  $\text{Cr}_{99}\text{Al}_1$  samples prepared on the fused silica substrates is above 400 K (and thus outside the measuring capabilities of the present experimental set-up), is in line with observations in previously reported [5, 6, 7, 9]. In studies [5, 6] performed on Cr and Cr-Ru thin films, the thin films deposited on fused silica also showed higher  $T_N$  values compared to samples deposited on single crystalline  $\text{MgO}(110)$  and  $\text{MgO}(100)$  substrates. These conclusions were confirmed in a later publication by Mudau *et al.* [7] where the residual stresses in Cr thin film samples used by Sheppard *et al.* [5] were investigated. The investigation revealed that the samples with enhanced  $T_N$  values were under tensile stresses of the order of 1 GPa [7]. Previous investigations [9] on polycrystalline Cr films, grown on Corning glass substrates, also show significant enhancement, up to 60 K above the bulk value, in  $T_N$  for  $t \leq 30$  nm. This is ascribed to internal tensile stresses in the films that arise, in part, from the grain boundaries [10, 11]. It is therefore probable to assume that the higher  $T_N$  values observed in the  $\text{Cr}_{99}\text{Al}_1$  thin films prepared on fused silica substrates could also be attributed to higher internal stress/strains in the coatings and will be the subject of a future study.

The present study therefore indicate that the crystallographic orientation influence the directional transport properties, as well as the  $T_N$  values of  $\text{Cr}_{99}\text{Al}_1$  thin films of various thicknesses. This is in line with results obtained in previous studies on thin magnetic films [4, 5, 6, 7, 8].

#### 4. Conclusions

XRD investigations of Cr<sub>99</sub>Al<sub>1</sub> thin films prepared on MgO(110), MgO(100) and fused silica substrates, with thickness 28.5 to 452 nm have been successful for structural characterization. The results indicated that the samples deposited on single crystalline substrates MgO(110) and MgO(100) are epitaxial and exhibit preferred growth direction, where-as those deposited on fused silica are polycrystalline. The  $T_N$  as function of  $t$  graphs for samples prepared on MgO(100) and MgO(110) show a decrease in the magnetic transition temperature with increase in thickness and the  $T_N$  values for the thickest samples being in good agreement with those found in bulk Cr<sub>99</sub>Al<sub>1</sub>. In the case of the fused silica samples, no  $T_N$  transitions were observed in the temperature range assessable with the equipment used. It is proposed that the higher  $T_N$  values in these samples are due to substantial tensile stresses in the coatings.

#### 5. Acknowledgements

The authors wish to thank the National Research Funding of South Africa (Grant numbers 80928; 80631 and 93551) and the Faculty of Science of the University of Johannesburg for financial support. The use of the analytical facility at UJ, Spectrum, is acknowledged. Necsa Limited SOC is acknowledged for the use of the XRD facilities within their User Program.

#### References

- [1] Fawcett E, Alberts HL, Galkin VY, Noakes DR and Yakhmi JV 1994 *Rev. Mod. Phys.* **66** 25
- [2] Sheppard CJ, Prinsloo ARE, Alberts HL, Muchono B and Strydom AM 2014 *J. Alloys Compd.* **595** 164
- [3] Baran A, Alberts HL, Strydom AM and P de V. du Plessis 1992 *Phys. Rev. B* **45** 10473
- [4] Zabel H 1999 *J. Phys. Condens. Matter* **11** 9303
- [5] Sheppard CJ, Prinsloo ARE, Fernando R R, Mudau ZP, Venter AM and Fullerton EE 2013 *SAIP Conf. Preceedings* 146
- [6] Prinsloo ARE, Derrett HA, Hellwig O, Fullerton EE, Alberts HL and Van den Berg N 2010 *J. Magn. Magn. Mat.* **322** 1126
- [7] Mudau ZP, Prinsloo ARE, Sheppard CJ, Venter AM, Ntsoane TP and Fullerton EE 2014 *SAIP Conf. Preceedings* 91
- [8] Mattson JE, Fullerton EE, Sowers CH and Bader SD 1995 *J. Vac. Sci. Technol. A* **13**(2) 276
- [9] Lourens JAJ, Aarajs S, Helbig HF, Cherlet L and Mehanna EA 1988 *J. Appl. Phys.* **63** 4282
- [10] Windischmann H 1992 *Crit. Rev. Solid State Mater. Sci.* **17** 547
- [11] Boekelheide Z, Helgren E and Hellman F 2007 *Phys. Rev. B* **76** 224429.